Electronic Supplementary Material (ESI) for New Journal of Chemistry.

Design, structures and study of non-covalent interactions of mono-, di-, and tetranuclear complexes of a bifurcated quadridentate tripod ligand, *N*-(aminopropyl)-diethanolamine

Farasha Sama[a], Istikhar A. Ansari[a], Mukul Raizada[a], Musheer Ahmad[b], C. M. Nagaraja[c], M. Shahid[a], Abhinav Kumar[d], Kulsum Khan[e], Zafar A. Siddiqi[a†]

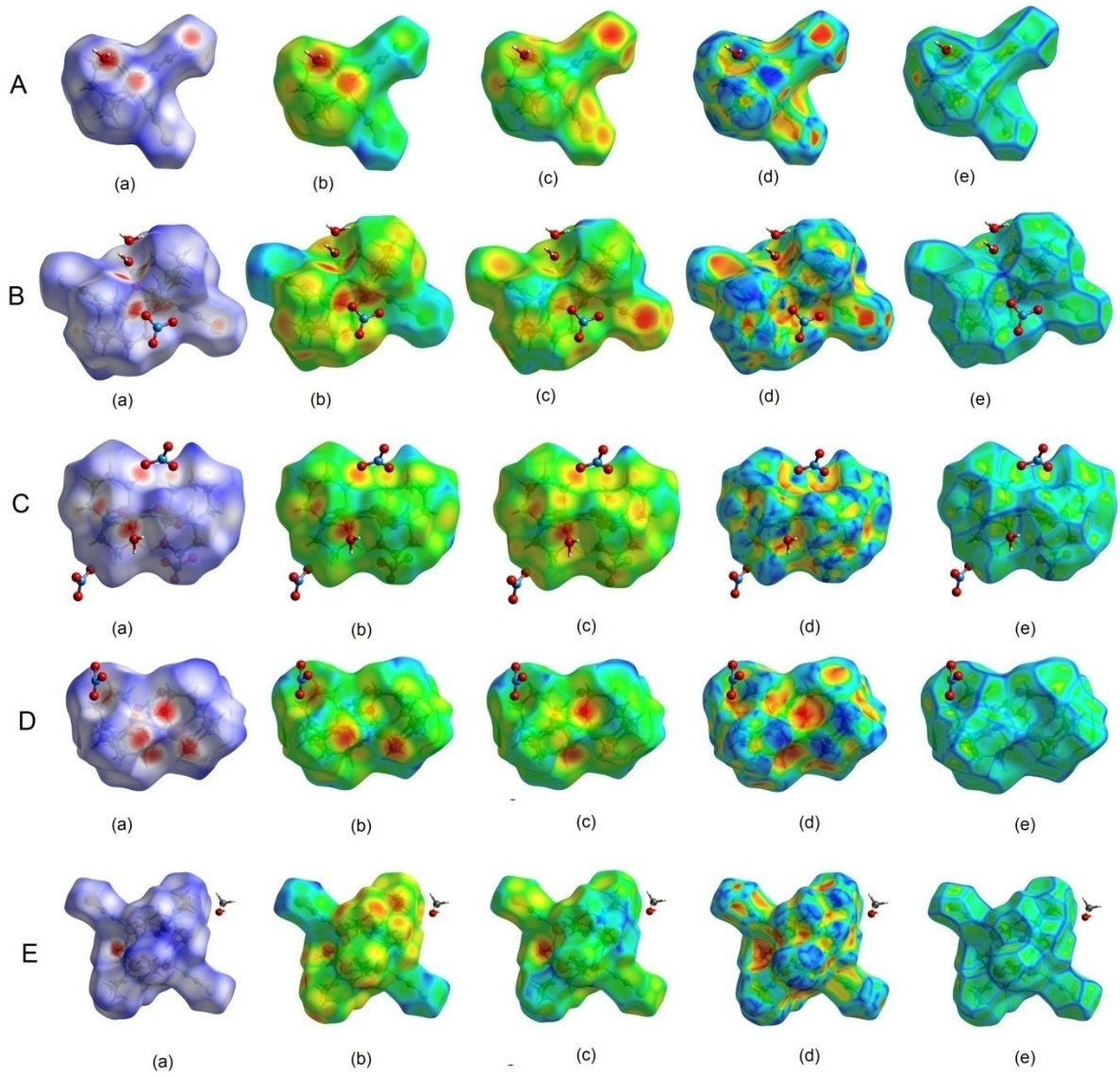

Fig. S1. Hirshfeld surfaces of **1** (A), **2** (B), **3** (C), **4** (D) and **5** (E) mapped with d_{norm} (a), d_i (b), d_e (c), shape index (d) and curvedness (e).

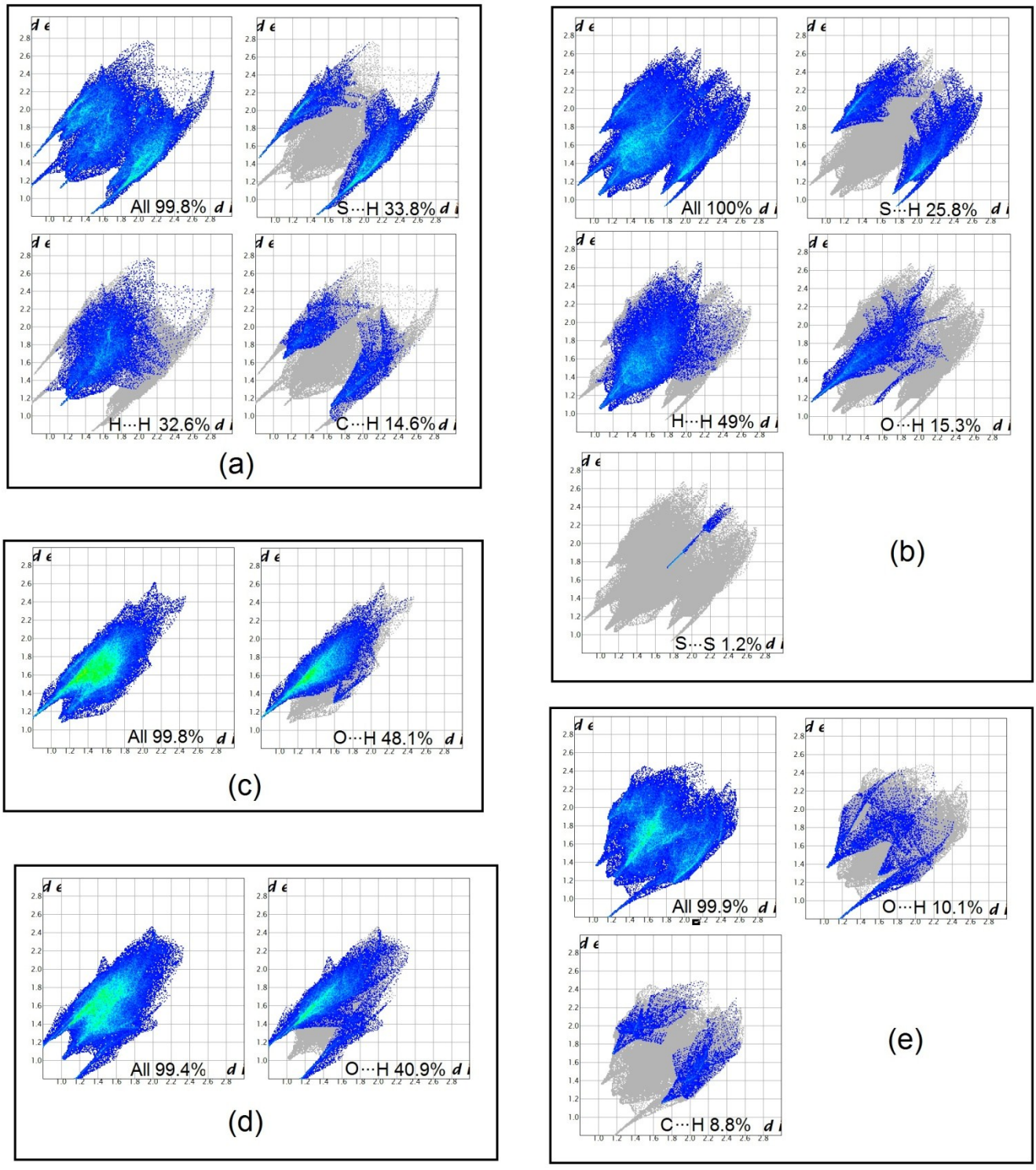

Fig.S2. The 2D-fingerprint plots of **1** (a), **2** (b), **3** (c), **4** (d) and **5** (e) showing different interactions.

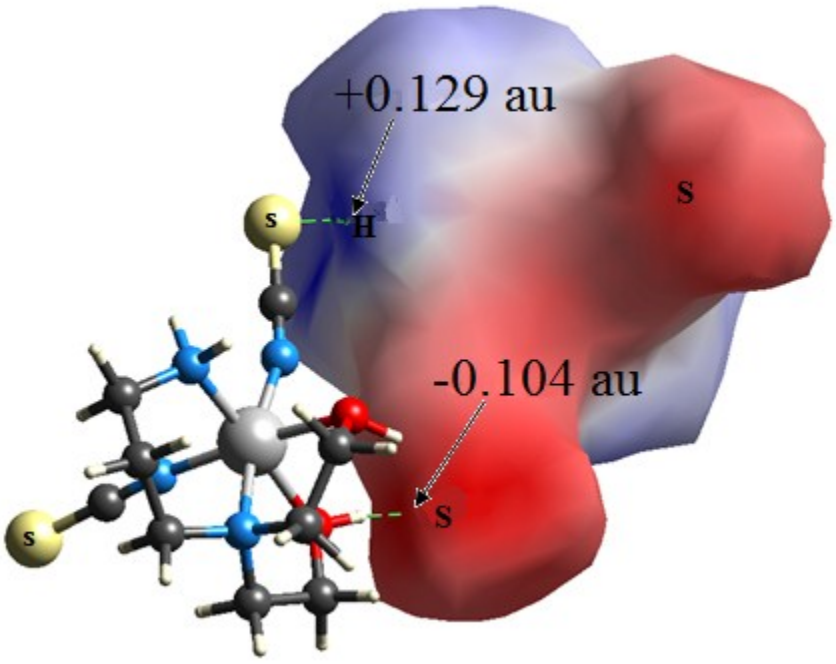

Fig. S3. Hirshfeld surface mapped with electrostatic potential (ESP) for **1**, showing the σ-hole on the non-protonated H atom of H_2apdea with potential values at two different interacting sites for S···H contacts.

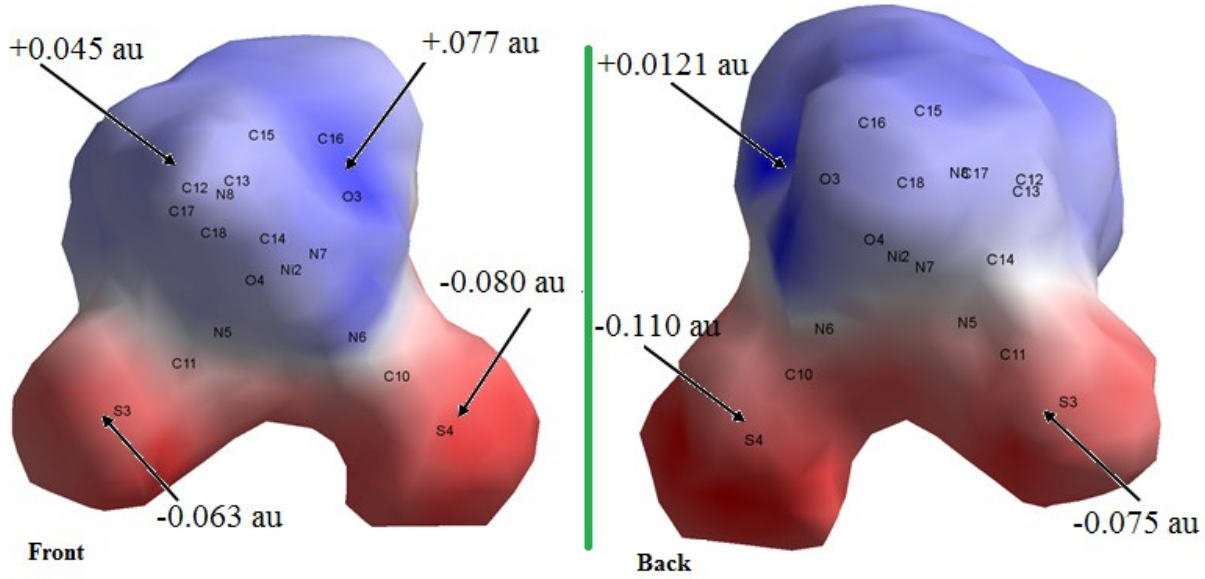

Fig. S4. Front and back views of the electrostatic potential (ESP) mapped over the Hirshfeld surface for **1** over the range −0.117 au (red) through 0.000 (white) to 0.159 au (blue).

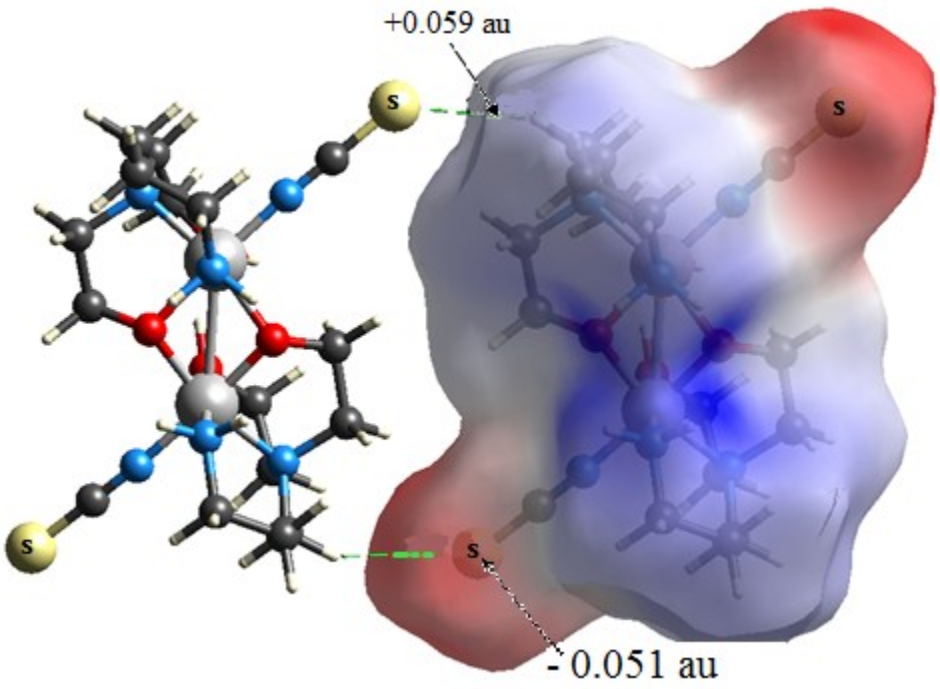

Fig. S5. Hirshfeld surface mapped with electrostatic potential (ESP) for **2**, showing the σ-hole on the H atom of Hapdea⁻ with potential values at two different interacting sites for S···H contacts.

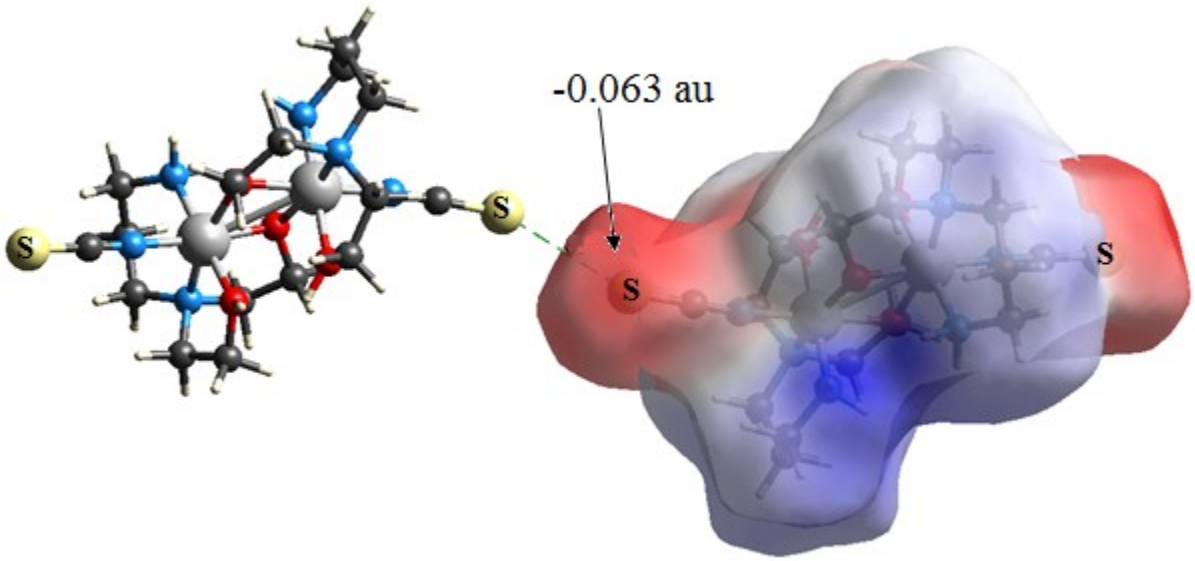

Fig. S6. Hirshfeld surface mapped with electrostatic potential (ESP) for **2**, showing the σ-hole on the H atom of Hapdea⁻ with potential value at interacting site for S···S contacts.

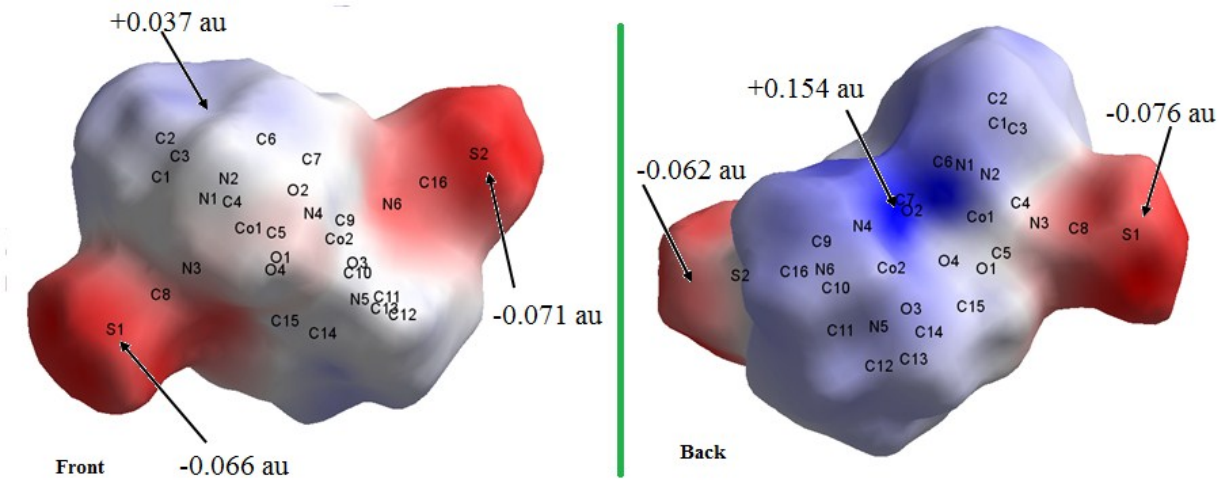

Fig. S7. Front and back views of the electrostatic potential (ESP) mapped over the Hirshfeld surface for **2** over the range −0.088 au (red) through 0.000 (white) to 0.163 au (blue).

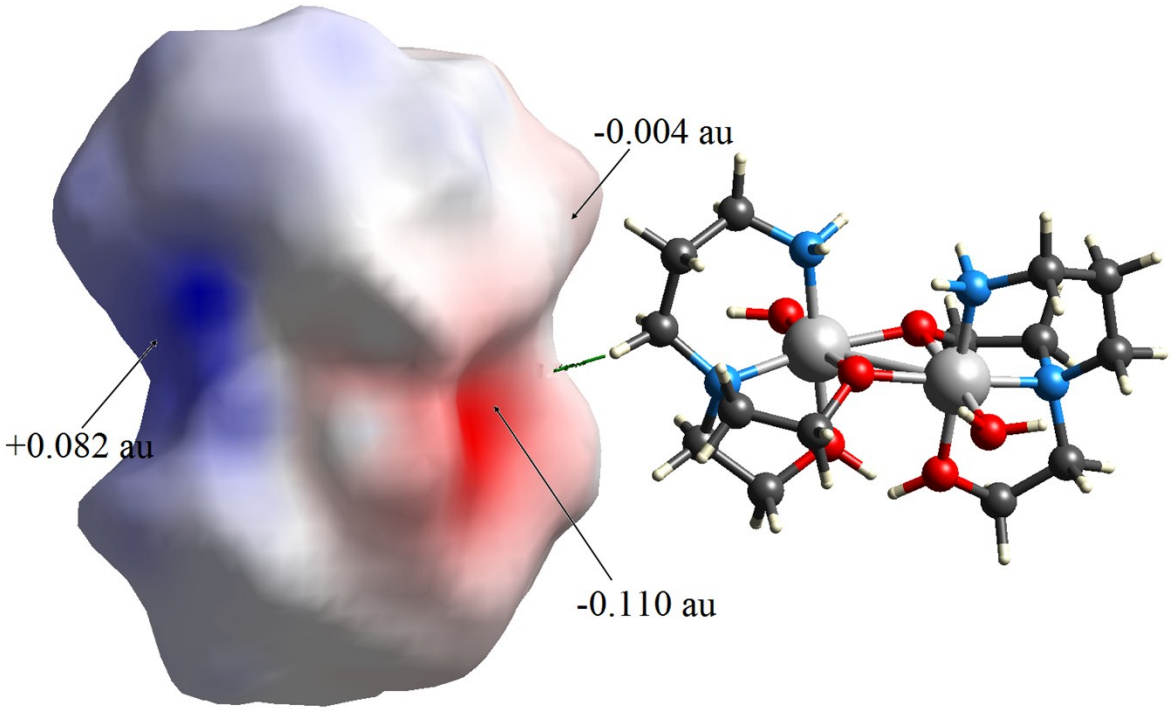

Fig. S8. Hirshfeld surface mapped with electrostatic potential (ESP) for **3**, showing the σ-hole on the mono-protonated H atom of Hapdea⁻ with potential value at interacting sites for O···H contacts.

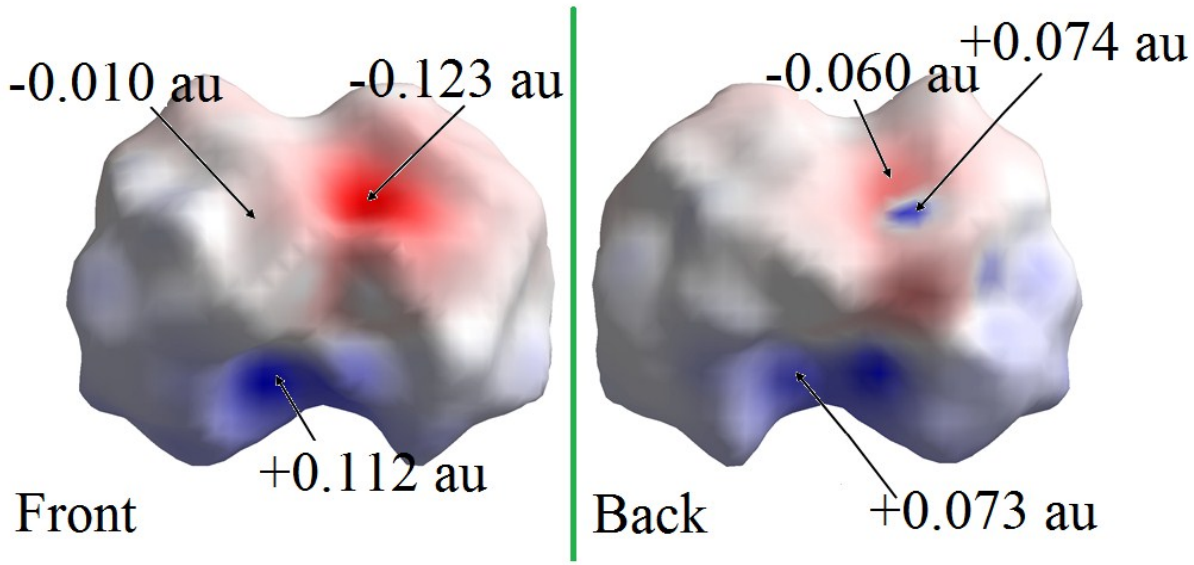

Fig. S9. Front and back views of the electrostatic potential (ESP) mapped over the Hirshfeld surface for **3** over the range −0.125 au (red) through 0.000 (white) to 0.120 au (blue).

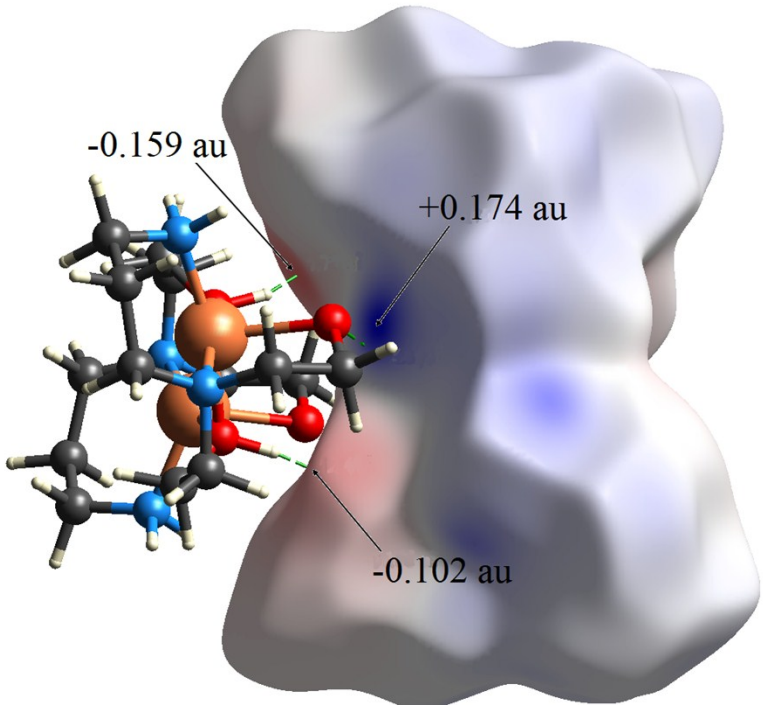

Fig. S10. Hirshfeld surface mapped with electrostatic potential (ESP) for **4**, showing the σ-hole on the H atom of $Hapdea^{-}$ with potential value at interacting sites for the O···H contacts.

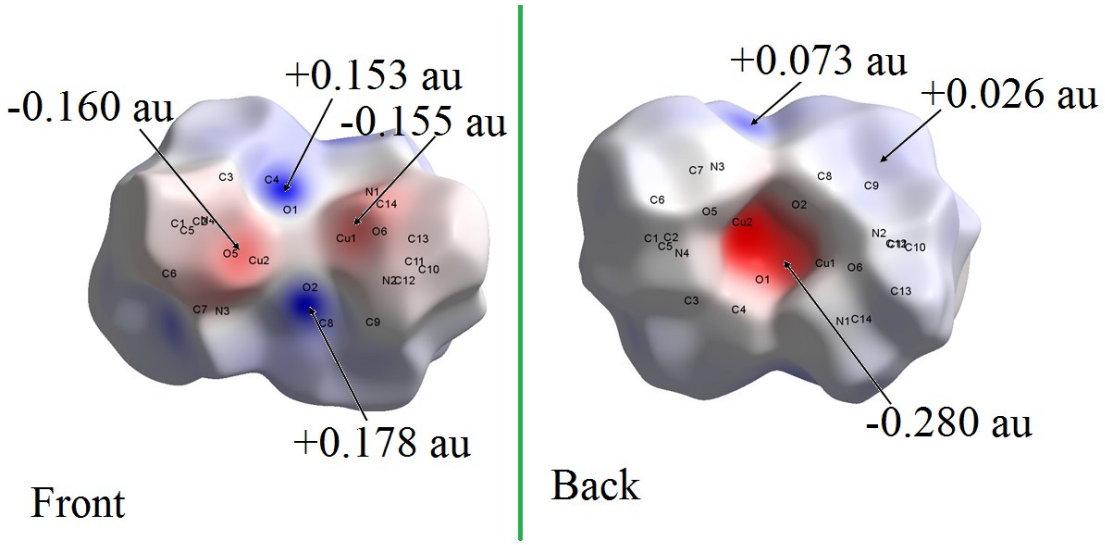

Fig. S11. Front and back views of the electrostatic potential (ESP) mapped over the Hirshfeld surface for **4** over the range −0.323 au (red) through 0.000 (white) to 0.179 au (blue).

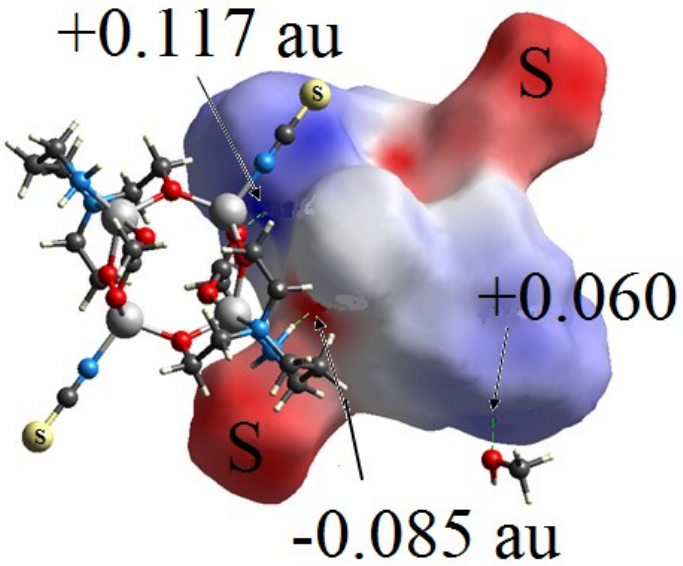

Fig. S12. Hirshfeld surface mapped with electrostatic potential (ESP) for **5**, showing the σ-hole on the non-protonated H atom of apdea^{2-} with potential value at interacting sites for O···H contacts.

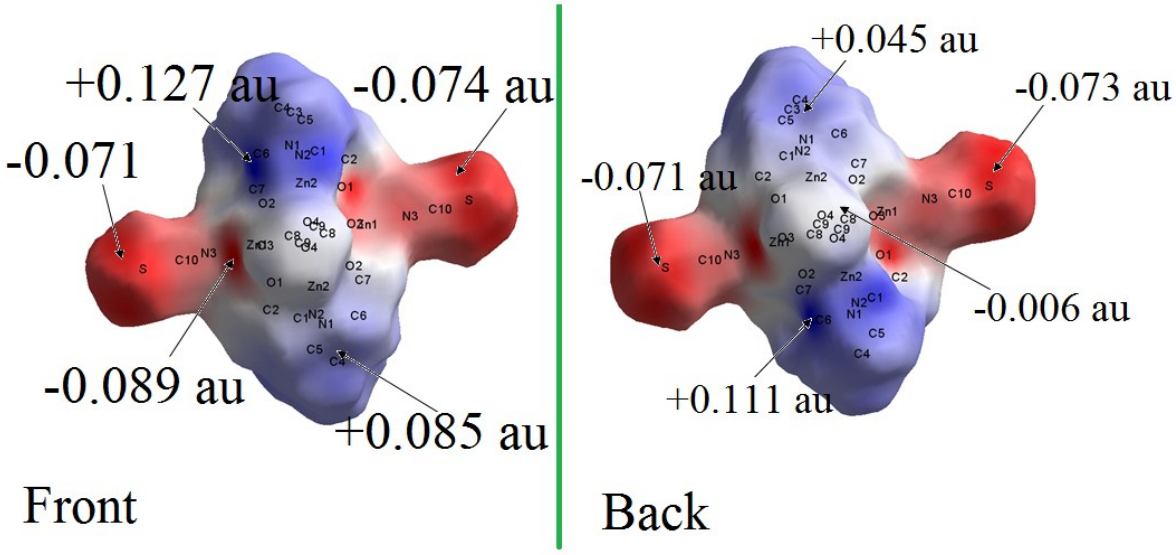

Fig. S13. Front and back views of the electrostatic potential (ESP) mapped over the Hirshfeld surface for **5** over the range −0.087 au (red) through 0.000 (white) to 0.120 au (blue).

Table S1. Selected bond lengths and angles for **1**.

Bond lengths		Bond angles	
N1 Ni1	2.015(4)	O1 Ni1 N3	81.25(14)
N4 Ni1	2.055(4)	O1 Ni1 O2	90.03(16)
N3 Ni1	2.110(4)	N2 Ni1 N1	93.41(15)
O2 Ni1	2.088(4)	N2 Ni1 N4	92.23(16)
O2 H2	0.76(5)	N2 Ni1 N3	93.67(15)
N5 Ni2	2.031(4)	N2 Ni1 O2	174.65(15)
N8 Ni2	2.052(5)	N2 Ni1 O1	87.56(16)
N7 Ni2	2.113(4)	N8 Ni2 N5	93.86(17)
O4 Ni2	2.116(4)	N7 Ni2 N5	92.77(16)
O4 H4	0.89(5)	N7 Ni2 N8	171.07(17)
O1 Ni1	2.146(4)	O4 Ni2 N5	87.43(16)
N2 Ni1	2.054(4)	O4 Ni2 N8	93.32(16)
O3 Ni2	2.132(4)	O4 Ni2 N7	81.00(15)
O3 H3	0.86(6)	O3 Ni2 N5	174.10(16)
N6 Ni2	2.046(4)	O3 Ni2 N8	91.91(15)
		O3 Ni2 N7	81.36(15)
		O3 Ni2 O4	90.99(16)
N4 Ni1 N1	92.70(16)	N6 Ni2 N5	92.05(17)
N3 Ni1 N1	170.15(15)	N6 Ni2 N8	91.47(16)
N3 Ni1 N4	93.86(15)	N6 Ni2 N7	94.27(15)
O2 Ni1 N1	91.46(16)	N6 Ni2 O4	175.20(15)
O2 Ni1 N4	89.77(15)	N6 Ni2 O3	89.04(16)
O2 Ni1 N3	81.23(15)	O1 Ni1 N4	175.08(15)
O1 Ni1 N1	92.22(15)		

Table S2. Selected bond lengths and angles for **2**.

Bond lengths		N2 Co1 N3	96.4(2)
Co1 Co2	2.9106(11)	N1 Co1 Co2	97.06(14)
Co1 O4	1.932(3)	N1 Co1 O4	88.76(17)
Co1 O2	1.890(3)	N1 Co1 O2	86.56(17)
Co1 O1	1.935(3)	N1 Co1 O1	178.99(18)
Co1 N3	1.890(4)	N1 Co1 N3	90.3(2)
Co1 N2	1.956(5)	N1 Co1 N2	95.50(19)
Co1 N1	1.947(4)	O4 Co2 Co1	40.93(10)
Co2 O4	1.889(3)	O2 Co2 Co1	39.91(9)
Co2 O2	1.939(3)	O2 Co2 O4	78.73(14)
Co2 O3	1.952(4)	O3 Co2 Co1	82.91(11)
Co2 N5	1.954(4)	O3 Co2 O4	93.43(15)
Co2 N4	1.929(5)	O3 Co2 O2	91.14(15)
Co2 N6	1.886(5)	N5 Co2 Co1	125.86(13)
Bond angles		N5 Co2 O4	87.54(16)
O4 Co1 Co2	39.82(9)	N5 Co2 O2	165.77(16)
O2 Co1 Co2	41.17(10)	N5 Co2 O3	85.89(17)
O2 Co1 O4	78.87(14)	N4 Co2 Co1	96.68(16)
O1 Co1 Co2	82.19(12)	N4 Co2 O4	87.2(2)
O1 Co1 O4	90.23(15)	N4 Co2 O2	87.6(2)
O1 Co1 O2	93.28(15)	N4 Co2 O3	178.4(2)
N3 Co1 Co2	135.29(16)	N4 Co2 N5	95.6(2)
N3 Co1 O4	96.76(18)	N6 Co2 Co1	135.81(16)
N3 Co1 O2	174.68(19)	N6 Co2 O4	175.36(18)
N3 Co1 O1	89.74(19)	N6 Co2 O2	97.32(18)
N2 Co1 Co2	126.33(13)	N6 Co2 O3	89.05(19)
N2 Co1 O4	166.10(16)	N6 Co2 N5	96.6(2)
N2 Co1 O2	88.16(17)	N6 Co2 N4	90.2(2)
N2 Co1 O1	85.49(17)	Co2 O4 Co1	99.24(15)

Table S3. Selected bond lengths and angles for **3**.

Bond lengths		N2 Co1 O2	178.33(11)
Co1 Co2	2.8853(5)	N2 Co1 O3	90.35(11)
Co1 O1	1.879(2)	N2 Co1 O4	88.09(9)
Co1 O2	1.917(2)	N2 Co1 N1	95.14(11)
Co1 O3	1.930(2)	O1 Co2 Co1	40.17(6)
Co1 O4	1.927(2)	O4 Co2 Co1	41.32(6)
Co1 N1	1.954(3)	O4 Co2 O1	79.15(8)
Co1 N2	1.939(2)	O5 Co2 Co1	82.89(6)
Co2 O1	1.9455(19)	O5 Co2 O1	90.94(8)
Co2 O4	1.878(2)	O5 Co2 O4	94.47(9)
Co2 O5	1.915(2)	O6 Co2 Co1	132.84(7)
Co2 O6	1.944(2)	O6 Co2 O1	94.29(9)
Co2 N3	1.953(2)	O6 Co2 O4	173.13(9)
Co2 N4	1.934(2)	O6 Co2 O5	87.63(10)
Bond angles		N3 Co2 Co1	126.08(8)
O1 Co1 Co2	41.90(6)	N3 Co2 O1	166.24(10)
O2 Co1 Co2	82.56(7)	N3 Co2 O4	87.78(10)
O2 Co1 O1	93.64(9)	N3 Co2 O5	85.78(10)
O3 Co1 Co2	134.14(7)	N3 Co2 O6	98.91(10)
O3 Co1 O1	175.15(9)	N4 Co2 Co1	97.94(8)
O3 Co1 O2	88.14(10)	N4 Co2 O1	87.52(9)
O4 Co1 Co2	40.06(6)	N4 Co2 O4	88.39(10)
O4 Co1 O1	79.61(8)	N4 Co2 O5	176.44(11)
O4 Co1 O2	91.38(9)	N4 Co2 O6	89.29(11)
O4 Co1 O3	95.85(9)	N4 Co2 N3	96.46(11)
N1 Co1 Co2	127.84(8)	Co2 O1 Co1	97.93(9)
N1 Co1 O1	88.85(10)	N1 Co1 O4	167.90(10)
N1 Co1 O2	85.70(10)	N2 Co1 Co2	98.02(7)
N1 Co1 O3	95.78(11)	N2 Co1 O1	87.82(10)

Table S4. Selected bond lengths and angles for **4**.

Bond lengths			
Cu1 Cu2	2.8893(5)	N1 Cu1 Cu2	124.12(7)
Cu1 O1	1.9694(19)	N1 Cu1 O1	85.36(8)
Cu1 O2	2.299(2)	N1 Cu1 O2	80.40(8)
Cu1 O3	1.9505(18)	N1 Cu1 O3	166.87(9)
Cu1 N2	1.987(2)	N1 Cu1 N2	94.11(10)
Cu1 N1	2.031(2)	O1 Cu2 Cu1	42.80(5)
Cu2 O1	1.9608(18)	O3 Cu2 Cu1	42.26(5)
Cu2 O3	1.9687(19)	O3 Cu2 O1	81.87(7)
Cu2 O4	2.324(2)	O4 Cu2 Cu1	111.73(5)
Cu2 N4	1.978(2)	O4 Cu2 O1	100.37(7)
Cu2 N3	2.026(2)	O4 Cu2 O3	93.38(8)
Bond angles		N4 Cu2 Cu1	134.83(8)
O1 Cu1 Cu2	42.57(5)	N4 Cu2 O1	98.52(9)
O2 Cu1 Cu2	117.38(6)	N4 Cu2 O3	171.54(10)
O2 Cu1 O1	97.12(8)	N4 Cu2 O4	94.85(10)
O3 Cu1 Cu2	42.75(5)	N3 Cu2 Cu1	124.80(7)
O3 Cu1 O1	82.11(7)	N3 Cu2 O1	167.19(9)
O3 Cu1 O2	104.99(8)	N3 Cu2 O3	85.34(9)
N2 Cu1 Cu2	132.09(7)	N3 Cu2 O4	80.96(9)
N2 Cu1 O1	168.01(9)	N3 Cu2 N4	94.04(10)
N2 Cu1 O2	94.59(9)	Cu2 O1 Cu1	94.64(8)
		N2 Cu1 O3	97.34(9)

Table S5. Selected bond lengths and angles for **5**.

Zn1 O1	1.945(3)	N3 Zn1 O1	105.94(15)
Zn1 O2	1.912(3)	N3 Zn1 O2	113.55(17)
Zn1 O3	2.004(3)	N3 Zn1 O3	103.93(17)
Zn1 N3	1.967(4)	O2 Zn2 O1	117.77(13)
Zn2 O1	1.987(3)	O4 Zn2 O1	97.20(13)
Zn2 O2	1.970(3)	O4 Zn2 O2	91.58(13)
Zn2 O4	2.147(3)	N1 Zn2 O1	84.78(13)
Zn2 N1	2.199(4)	N1 Zn2 O2	83.00(13)
Zn2 N2	2.031(4)	N1 Zn2 O4	174.53(13)
Bond angles		N2 Zn2 O1	117.45(14)
O2 Zn1 O1	121.50(13)	N2 Zn2 O2	124.52(15)
O3 Zn1 O1	104.98(14)	N2 Zn2 O4	86.67(15)
O3 Zn1 O2	105.26(14)	N2 Zn2 N1	96.97(15)
Zn2 O1 Zn1	128.63(15)		

Table S6. Selected geometries of non-covalent interactions in **1**–**5**.

D–H···A	d(D–H)	d(H···A)	d(D···A)	∟(DHA)
(**1**)				
N2–H2···S4	0.899	2.727	3.340	126.30
O1–H1···S2	0.700	2.518	3.193	162.62
C5–H5···C2	0.970	2.690	3.647	168.93
(**2**)				
C3–H3···S1	0.971	2.894	3.790	153.85
C15–H15···O7	0.971	2.595	3.377	137.71
N4–H4···O6	0.801	2.403	3.159	157.92
N1–H1···O5	0.900	2.123	3.008	167.61
C15–H15···O7	0.970	2.595	3.377	137.71
(**3**)				
C12–H12···H9	0.970	2.541	3.471	160.63
O6–H6···O8	0.850	2.048	2.762	141.11
N4–H4···O8	0.900	2.111	2.964	157.84
N2–H2···O7	0.900	2.456	3.316	159.98
O6–H6···O16	0.850	1.786	2.619	168.91
(**4**)				
O4–H4···O5	0.865	1.865	2.725	172.99
O6–H6···O1	0.859	1.790	2.645	173.38
O8–H8···O3	0.857	1.855	2.706	171.61
C17–H17···O20	0.970	2.635	3.595	170.39
C24–H24···O19	0.970	2.576	3.512	162.22
C21–H21···O18	0.970	2.410	3.150	132.82
N4–H4···O12	0.900	2.207	3.093	167.93
N2–H2···O3W	0.900	2.349	3.119	143.53
(**5**)				
N2–H2···C10	0.900	2.795	3.390	124.70
N2–H2···O3	0.900	2.229	3.127	175.89
C3–H3···O5	0.971	2.496	3.382	151.61
O5–H5···O1	0.819	1.999	2.814	172.92
O5–H5···C2	0.819	2.742	3.451	145.82

Table S7. Bond valence summation (BVS) calculations for **2** and **3**.

Complex	Metal atom	BVS	
		Co(II)	Co(III)
(**2**)	Co1	3.316	***2.959***
	Co2	3.318	***2.963***
(**3**)	Co1	3.279	**2.891**
	Co2	3.246	**2.864**

Table S8. Magnetic data and calculations

Complex	Magnetic moments, μ_{eff} (B.M.)*	
	Observed*	Calculated**
1	2.84	2.82
2	8.90	8.94
3	8.88	8.94
4	2.83	2.82
5	0	0

*The data are collected using magnetic susceptibility balance which contains a pair of magnets mounted at opposite ends of a beam, initially in equilibrium and when sample is introduced into the balance, a disruption of the magnetic field results. A current through a coil situated between the poles of a second pair of magnets returns the beam to equilibrium. The current through the coil is measured and transformed into a numerical reading. Diamagnetic materials are weakly repelled by an external magnetic field, resulting in a negative reading. Paramagnetic materials are attracted to an external magnetic field and give a positive reading. The magnetic analysis supported the mixed valence states of the cobalt ions in the clusters. The magnetic moment of the complexes was calculated using by the formula as follows:

$\chi_{g} = LC_{bal}(R - Ro)/10^{9}(m)$

L = height of sample in tube in units of centimeters, C_{bal} = balance calibration constant = 1.0, R = reading for tube plus sample

R_o = reading for the empty tube, m = mass of the sample in units of grams

The molar magnetic susceptibility is then calculated from the gram magnetic susceptibility using the following equation:

$\chi_m = \chi_g \times (molar\ mass)$

$\chi_A = \chi_m$ – diamagnetic correction

The magnetic susceptibility for a particular substance is not particularly useful in itself. However, the effective magnetic moment for a particular substance can be calculated from the gram magnetic susceptibility using the following equation.

$\mu_{eff} = 2.283\sqrt{\chi_A.T}\ B.M.$

{χ_g=magnetic susceptibility in erg.G^{-2}.gm^{-1}, χ_m=molar susceptibility in erg.G^{-2}.mol^{-1}, and μ_{eff} = effective magnetic moment in B. M.}.

**$\mu_{eff} = \{n(n+2)\}^{1/2}$, n = no. of unpaired electron